

Article

High-Durability Concrete with Supplementary Cementitious Admixtures Used in Corrosive Environments

Shiming Liu ¹, Miaomiao Zhu ^{1,*}, Xinxin Ding ^{1,2}, Zhiguo Ren ³, Shunbo Zhao ^{1,2,*} , Mingshuang Zhao ¹  and Juntao Dang ¹

¹ International Joint Research Lab for Eco-Building Materials and Engineering of Henan, School of Civil Engineering and Communications, North China University of Water Resources and Electric Power, Zhengzhou 450045, China; liushm@ncwu.edu.cn (S.L.); dingxinxin@ncwu.edu.cn (X.D.); zhaomingshuang@stu.ncwu.edu.cn (M.Z.); dangjuntao@ncwu.edu.cn (J.D.)

² Collaborative Innovation Center of New Urban Building Technology of Henan, North China University of Water Resources and Electric Power, Zhengzhou 450045, China

³ Zhuzhou China Railway Electrical Materials Co. LTD., Zhuzhou 412001, China; zhaoms@stu.ncwu.edu.cn

* Correspondence: zhumm@stu.ncwu.edu.cn (M.Z.); sbzhao@ncwu.edu.cn (S.Z.); Tel.: +86-371-65665160 (S.Z.)

Abstract: Durability of concrete is of great significance to prolong the service life of concrete structures in corrosive environments. Aiming at the economical and environment-friendly production of concrete by comprehensive utilization of the supplementary cementitious materials made of industrial byproducts, the resistances to chloride penetration, sulfate attack, and frost of high-performance concrete were studied in this paper. Fifteen concretes were designed at different water–binder ratio with the changes of contents of fly ash (FA), silica fume (SF), ground granulated blast-furnace slag (GGBS), and admixture of sulfate corrosion-resistance (AS). The compressive strength, the total electric flux of chloride penetrability, the sulfate resistance coefficient, and the indices of freezing and thawing were measured. Results indicate that, depending on the chemical composition, fineness, and pozzolanic activity, the supplementary cementitious admixtures had different effects on the compressive strength and the durability of concrete; despite having a higher fineness and pozzolanic activity, the GGBS gave out a negative effect on concrete due to a similar chemical composition with cement; the SF and FA presented beneficial effects on concrete whether they were used singly with GGBS or jointly with GGBS; the AS improved the compressive strength and the sulfate corrosion resistance of concrete. In general, the grade of durability was positively related to the compressive strength of concrete. Except for the concretes admixed only with GGBS or with GGBS and FA, others had super durability with the compressive strength varying from 70 MPa to 113 MPa. The concretes with water to binder ratio of 0.29 and total binders of 500 kg/m³ admixed with 7% FA + 8% SF + 8% GGBS or 7% FA + 8% SF + 8% GGBS + (10–12)% AS presented the highest grades of resistances specified in China codes to chloride penetration, sulfate corrosion, and frost, while the compressive strength was about 100 MPa.

Keywords: high-durability concrete; fly ash; silica fume; ground granulated blast-furnace slag; sulfate corrosion inhibitor; compressive strength; chloride penetration; sulfate corrosion; freezing and thawing



Citation: Liu, S.; Zhu, M.; Ding, X.; Ren, Z.; Zhao, S.; Zhao, M.; Dang, J. High-Durability Concrete with Supplementary Cementitious Admixtures Used in Corrosive Environments. *Crystals* **2021**, *11*, 196. <https://doi.org/10.3390/cryst11020196>

Academic editors: Sławomir J. Grabowski and Piotr Smarzewski
Received: 21 January 2021
Accepted: 15 February 2021
Published: 17 February 2021

Publisher's Note: MDPI stays neutral with regard to jurisdictional claims in published maps and institutional affiliations.



Copyright: © 2021 by the authors. Licensee MDPI, Basel, Switzerland. This article is an open access article distributed under the terms and conditions of the Creative Commons Attribution (CC BY) license (<https://creativecommons.org/licenses/by/4.0/>).

1. Introduction

Concrete is the most widely used building material in the world. The degradation of material properties caused by environmental effects will affect the durability of concrete in the process of using concrete structures. The lack of durability of concrete will not only affect the normal use of the project and prematurely terminate the service life of the structure, but also increase the maintenance cost during use and cause serious waste of resources [1]. Therefore, the preparation of high-performance concrete with excellent durability is of great significance to improve the service life of building structures. The

additional benefit is to promote the transformation and development of the construction industry.

Normally, the issue of durability of concrete structures is caused by the chloride penetration, sulfate corrosion, or frost damage. The chloride that penetrates into concrete through pores and microcracks results in the corrosion of reinforcement, further damage, and the cracking and spalling of concrete cover, and will take place due to the volume expansion of corroded products. Finally, structural damage happens with the loss of bond between reinforcement and concrete [2,3]. Sulfate corrosion is a complicated process of physical, chemical, and mechanical changes. The sulfate ions enter firstly into the pores of concrete, then the chemical reaction comes up between sulfate ions and cement hydration products to cause the crystallization precipitation of corrosive substances. The expansion of corrosion products leads to the damage of cracking, spalling, and strength loss of concrete [4–6]. For concrete subjected to the action of freezing and thawing, the degradation of concrete happens due to the continuous extending of the pores with repeated freeze–thaw of the free moisture [7].

Different measures have been used to improve the durability of concrete, in which an effective method is the use of supplementary cementitious admixtures in concrete. Fly ash (FA), silica fume (SF), ground granulated blast-furnace slag (GGBS), and other mineral admixtures of industrial byproducts are always applied to concrete by replacing parts of Portland cement. This not only aims at the reduction of energy consumption of cement production, but also comprehensively realizes the industrial sustainability with lower carbon emission. The functions of supplementary cementitious admixtures are the pozzolanic effect and the filling effect. The benefits are the refining of the pore structure, the improving of the interface transition zone, and the increase in density of concrete [8,9]. However, due to the different mineral compositions, chemical activity, and physical properties, as well as forming processes of different cementitious admixtures, the concrete with single mineral admixture has some shortcomings [10]. It is well known that concrete with FA has such advantages as reduction of hydration heat, restraint of alkali–silicate reaction, long-term development of strength, and improvement of durability [6,11]. However, the problems are difficult to avoid, including the easier carbonation, the necessity of long curing duration, the slower development of strength, and the heterogeneity [12,13]. The strength and long-term durability of concrete can be effectively improved by admixing SF, while the risk exists in the increasing of water demand and shrinkage of concrete [3,14–17]. GGBS, with a main component of vitreous, is a kind of auxiliary cementitious material with potential activity. The potential activity can be motivated by $\text{Ca}(\text{OH})_2$ produced by cement hydration, and well developed in the later hydration stage. Meanwhile, the supplementary cementitious admixtures have a significant impact on the resistance of concrete to chloride penetration, due to the chloride-binding capacity of these materials. That is, chloride ions can react with C_3A and C_4AF to the stable forms $3\text{CaO}\cdot\text{Al}_2\text{O}_3\cdot\text{CaCl}_2\cdot 10\text{H}_2\text{O}$ and $3\text{CaO}\cdot\text{Fe}_2\text{O}_3\cdot\text{Al}_2\text{O}_3\cdot\text{CaCl}_2\cdot 10\text{H}_2\text{O}$ to decrease the free chlorides [18].

In the design of high-performance concrete, it is necessary to take into account the optimization of a variety of performance indicators. This provides opportunities for the hybrid uses of different kinds of supplementary cementitious admixtures. The synergistic action of multi-component cement is significant, if the blender could have a wider particle size distribution, a highly reactive pozzolan that would consume the $\text{Ca}(\text{OH})_2$ released by the early hydration of ordinary Portland cement, and a latent pozzolan that would consume the $\text{Ca}(\text{OH})_2$ released at a later stage [10]. As reported for a ternary concrete containing 20% FA + 7.5% SF with the water to binder ratio (w/b) of 0.3, the resistance of chloride penetration increased significantly, with the index of total electric flux reduced by 78.0%; however, the compressive strength reduced by 5.7% compared with the reference concrete [14]. As studied by Elahi et al. [11], the total electric flux of chloride penetration test was reduced by 88.7% without affecting the compressive strength for the ternary concrete containing 40% FA + 10% SF with $w/b = 0.32$, and the total electric flux was decreased by 92.7% with the increase of compressive strength by 5.8% for the ternary concrete containing

7.5% SF + 50% GGBS. The study of Wu et al. [19] indicated that the total electric flux of chloride penetration test for ternary concrete with 10% FA + 20% GGBS, 15% FA + 15% GGBS, and 20% FA + 10% GGBS decreased by 44.8%, 60.5% and 55.8%, respectively, and the relative dynamic elastic modulus after 300 freezing and thawing cycles of frost test increased to 87.3%, 90.1%, and 84.9% from 58.4% of reference concrete. Additionally, the quaternary concrete with three mineral admixtures was studied by Yan et al. [20]. In condition of the $w/b = 0.33$, the compressive strength and the sulfate resistance of concrete with 10% FA + 10% SF + 5% GGBS was the same as those of reference group; the compressive strength and the corrosion resistance of concrete with 15% FA + 15% SF + 10% GGBS increased by 15.2% and 5.0%, respectively. Therefore, the shortcomings of multi-component concrete can be compensated by the collaborative optimization of several admixtures.

In recent years, the admixtures of sulfate corrosion-resistance (AS) have been developed. The respective functions of expansion, excitation, filling, and water-reducing are provided by the components of AS to resist the salt erosion. The AS was prepared by Yang [21] using the anhydrite (CaSO_4), the ultra-fine slag powder, and the anhydrous calcium sulfoaluminate (CSA). The experimental results show that the AS can significantly improve the resistances of concrete to chloride penetration, sulfate corrosion, and carbonation. Meanwhile, other research also shows that AS can effectively promote the hydration of cement [22], improve the pore structure of concrete with reduced porosity [23], and increase the density of concrete [24]. This comprehensively improves the performance of concrete.

With the needs of corrosion determination, test methods are specified in related test codes [25,26]. Meanwhile, different methods were innovated to research the corrosion mechanisms of concrete. For instance, the thermal analysis method for attack products and the chemical titrating method for sulfate ion content were developed for the concrete in sulfate corrosion [27], and the non-destructive testing measurements, including ground penetrating radar, were used to detect the damage of corroded concrete [28]. This is an important research aspect dealing with the issues of test methodology.

Based on the above analyses, the research of this paper is concentrated on the preparation of high-durability concrete with supplementary cementitious materials. It aims at the economical and environment-friendly production of concrete by comprehensive utilization of industrial byproducts. Combined with the durability requirement of concrete structures built in severe environments, a high-performance concrete with multiple resistances to chloride penetration, sulfate corrosion, and frost was developed. The supplementary cementitious admixtures of FA, SF, GGBS, and AS were used in binary and ternary combinations. Fifteen mix proportions of concrete were designed and prepared for the experimental study. The results are discussed with the explanation of the admixtures' effects on internal structure of concrete, and the mix proportions of concrete are selected to produce high-durability concrete in engineering applications.

2. Materials and Test Methods

2.1. Materials

The cement was grade P·O 42.5 ordinary Portland cement produced by Xinhua Cement Co. Ltd. Hubei, China. The supplementary cementitious admixtures were the fly ash (FA), silicate fume (SF), ground granulated blast-furnace slag (GGBS), and admixture of sulfate corrosion-resistance (AS). Their chemical compositions are presented in Table 1, of which LOI is the loss on ignition. The physical and mechanical properties of cement are presented in Table 2, which meet the relevant specifications of China codes GB 175 [29]. The physical and mechanical properties of FA, SF, GGBS, and AS are presented in Table 3, which meet the relevant specifications of China codes GB/T 1596, GB/T 27690, GB/T 18046, and JC/T 1011 [30–33].

Table 1. Chemical compositions of cement, fly ash (FA), silica fume (SF), ground granulated blast-furnace slag (GGBS), and admixture of sulfate corrosion-resistance (AS).

Materials	Chemical Compositions (%)									
	SiO ₂	Fe ₂ O ₃	Al ₂ O ₃	CaO	MgO	SO ₃	f-CaO	K ₂ O	K ₂ O	LOI
cement	21.6	3.3	4.9	56.4	3.4	2.2	0.9	0.1	0.1	5.3
FA	55.9	5.9	17.3	6.6	3.8	1.9	0.3	1.9	1.9	2.6
SF	88.3	0.7	0.9	1.2	0.2	0.9	0.3	0.7	0.7	0.8
GGBS	25.9	2.6	8.4	41.4	4.5	0.1	0.1	0.5	0.5	4.0
AS	48.0	2.4	8.6	20.3	1.9	7.4	3.7	0.6	0.6	1.9

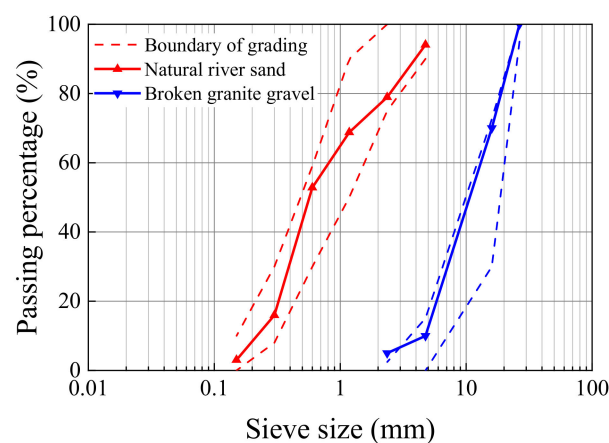
Table 2. Physical and mechanical properties of ordinary Portland cement.

Density (kg/m ³)	Fineness (m ² /kg)	Setting Time (min)		Flexural Strength (MPa)		Compressive Strength (MPa)	
		Initial	Final	3d	28d	3d	28d
3133	324	236	308	5.1	7.8	24.9	47.2

Table 3. Physical and mechanical performances of FA, SF, GGBS, and AS.

Materials	Density (kg/m ³)	Fineness (m ² /kg)	Water Demands Ratio(%)	Active Index (%)	
				7d	28d
FA	2342	406	84	—	73.3
SF	2149	—	101.7	97.8	—
GGBS	2998	438.8	—	76	97.6
AS	2703	380	—	95	102

The fine aggregate was river sand with a fineness modulus of 2.86 and an apparent density of 2640 kg/m³. The coarse aggregate was crushed granite gravel with continuous grading and a maximum particle of 20 mm, and an apparent density of 2730 kg/m³. As presented in Figure 1, the gradations of fine and coarse aggregates met the specifications of China codes GB/T 14684 and GB/T14685 [34,35]. The polycarboxylate-based superplasticizer (PS) was used with water-reducing rate of 27% and solid content of 23%. The mixing water was tap water.

**Figure 1.** Grading of fine and coarse aggregates.

2.2. Mix Proportion

To study the effects of supplementary cementitious admixtures on the compressive strength and durability of concrete, fifteen mix proportions were designed by the absolute

volume method in accordance with China code JGJ 55 [36]. FA and SF were mainly used to adjust the w/b , while GGBS and AS replaced cement to keep the constant of w/b . The content of PS in the percentage of the total mass of cementitious materials was adjusted by trial mixing to keep the slump of the fresh concrete at (70 ± 20) mm. Table 4 presents the confirmed mix proportions of test concretes, of which the first letters of SF, GGBS, FA, and AS are used respectively to identify the materials.

Table 4. Mix proportions of high-performance concrete.

Identifier of Mixture	w/b	Dosage of Raw Materials (kg/m ³)						PS (%)	
		Cement	FA	SF	GGBS	AS	Sand		Gravel
S1-1	0.33	425	0	14	0	0	721.0	1227.6	2.6
G1-1	0.33	425	0	0	14	0	674.8	1253.2	1.6
S1G2-1	0.33	385	0	14	40	0	715.1	1217.5	2.4
F1S2-2	0.29	425	35	40	0	0	697.1	1187.0	2.2
F1G2-2	0.29	425	35	0	40	0	652.5	1211.8	1.8
F1S2G2-2	0.29	385	35	40	40	0	691.2	1177.0	2.2
F2S3-3	0.25	425	55	100	0	0	668.3	1138.0	2.2
F2G3-3	0.25	425	55	0	100	0	625.6	1161.8	1.8
F2S3G2-3	0.25	385	55	100	40	0	662.4	1127.9	2.4
F1S2A1-2	0.29	375	35	40	0	50	657.7	1221.5	3.0
F1G2A1-2	0.29	375	35	0	40	50	650.1	1207.4	2.0
F1S2G2A1-2	0.29	335	35	40	40	50	652.1	1211.1	2.8
F1S2A2-2	0.29	365	35	40	0	60	657.2	1220.6	2.8
F1G2A2-2	0.29	365	35	0	40	60	649.6	1206.5	2.2
F1S2G2A2-2	0.29	325	35	40	40	60	651.6	1210.2	2.8

2.3. Test Method

The mixtures of concrete were mixed with a horizontal-shaft mixer, and the specimens were fabricated in molds and compacted on a vibrating table. All specimens were demolded after 24 h and cured in a standard curing room with a temperature of (20 ± 2) °C and relative humidity of 95% for 56 days before testing.

The test for compressive strength was in accordance with China code GB/T 50081 [37]. The specimen was a cube with a dimension of 100 mm. As the cubic compressive strength (f_{cu}) is corresponding to the standard cube with a dimension of 150 mm, the test value was converted by multiplying a coefficient of 0.95. The loading rate was 0.8 MPa/s on the tested cube by a compression-testing machine.

Tests for chloride ion penetration, sulfate corrosion, and rapid freezing and thawing were in accordance with China code GB/T 50082 [25]. The first one is the electric flux test, which is similar to the test method specified in ASTM C1202 [38]. The samples of $\phi 100$ mm \times 50 mm for chloride ion penetration test was cut from the specimen of $\phi 100$ mm \times 200 mm. The test procedure was as follows: (1) The sample was put into a vacuum to be water saturated; (2) the samples were installed into the testing cell, ensuring the reliable sealing of the sample with the testing cell; (3) 0.3 M NaOH solution and 3% NaCl solution were placed in the testing cells on two sides of the sample, respectively, and connected to the positive and negative terminals of the power supply; (4) the DC power was switched on, and the total electric flux passed through the sample was automatically recorded for 6 h. Finally, the measured total electric flux (Q_{100}) was converted to become the value (Q_s) as a standard sample with diameter of 95 mm, that is,

$$Q_s = Q_{100} \times \left(\frac{95}{100} \right)^2 \quad (1)$$

Three groups of cubic specimens with a dimension of 100 mm were used for the sulfate resistance test of the same concrete. One group was used for the reference cured at the standard conditions. Another two were for the test of sulfate resistance as per the

following procedure: (1) put the specimens into the oven to be dried at $(80 \pm 5)^\circ\text{C}$ for 48 h and cool down to room temperature; (2) move the specimens into the sulfate solution with 5% Na_2SO_4 of automatic sulfate dry–wet cycle testing machine. One group went through 120 dry–wet cycles, another went through 150 dry–wet cycles. A cycle included the soaking in solution for 15 h, heating to 80°C after draining the solution, maintaining at the temperature of $80 \pm 5^\circ\text{C}$ for 5 h, and cooling after drying. Each cycle lasted for about (24 ± 2) h. The corrosion resistance coefficient (K_f) was computed by the compressive strength ratio of the sulfate corroded to reference specimens, as follows:

$$K_f = \frac{f_{cn}}{f_{c0}} \quad (2)$$

where f_{cn} is the compressive strength of specimens after sulfate corrosion for n dry–wet cycles; f_{c0} is the compressive strength of reference specimens at the same time.

Before the rapid freezing and thawing test, the prismatic specimens of $100\text{ mm} \times 100\text{ mm} \times 400\text{ mm}$ were immersed in water with a temperature of $(20 \pm 2)^\circ\text{C}$ for 4 days, and the initial value of fundamental frequency (f_0) and initial value of weight (W_0) of the specimens were measured. Then, the specimens were put into the freeze–thaw testing machine. Each cycle of freezing and thawing was completed within 5–6 h, in which the melting time was not less than one quarter of the total freeze–thaw time. The fundamental frequency (f_n) and the weight (W_n) of specimens were measured for each of 25 cycles of freezing and thawing. The relative dynamic elastic modulus (P_n) and the weight loss rate (ΔW_n) were calculated as follows:

$$P_n = \frac{f_n^2}{f_0^2} \times 100 \quad (3)$$

$$\Delta W_n = \frac{W_0 - W_n}{W_0} \times 100 \quad (4)$$

3. Results and Discussion

3.1. Compressive Strength

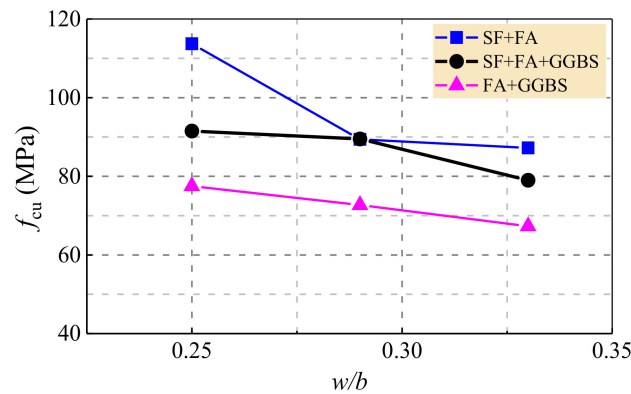
Test results of compressive strength are presented in Table 5. Comparing groups of S1-1 with G1-1, F1S2-2 with F1G2-2, and F2S3-3 with F2G3-3, the compressive strength ratios are 1.30, 1.23, and 1.47. This indicates that, due to the higher activity, as presented in Table 3, the SF has a higher strengthening effect than GGBS in the same conditions. As we know, the high activity of SF comes from the amorphous silica with high volcano ash activity that can react with $\text{Ca}(\text{OH})_2$, a cement hydration product, to form a calcium–silicate–hydrate (C–S–H) gel [14–17].

As presented in Tables 1 and 3, the chemical composition and pozzolanic activity of GGBS were similar to cement, therefore, the hydration reaction of GGBS and cement was basically equivalent. Theoretically, replacing equal weight of cement by GGBS should not lead to an obvious decrease in the concrete strength. Comparing with group S1-1, the compressive strength of S1G2-1 reduced about 10%. However, this also depends on the joint admixing and contents of FA and SF. Comparing groups F1S2-2 with F1S2G2-2, and F2S3-3 with F2S3G2-3, the compressive strength ratios are 1.00 and 1.24. This indicates that with proper contents of SF and FA, the secondary hydration of SF and FA with $\text{Ca}(\text{OH})_2$ released from the hydration of cement could come up to a sufficient status, and the strength of concrete could remain unchanged by replacing 40 kg/m^3 cement with GGBS. When the content of SF was much higher than FA, the insufficient secondary hydration of SF and FA took place with a competition for $\text{Ca}(\text{OH})_2$. This led to the obviously reduced strength of concrete with the replacing of 40 kg/m^3 cement with GGBS. In the last condition of F2S3G2-3, the SF could not release the potential activity during the hardening of concrete.

Table 5. Test results of compressive strength and resistances to chloride penetration and sulfate attack.

Identifier of Mixtures	f_{cu} (MPa)	Q_s (C)	f_{cu} at 120 Times Cycle (MPa)		K_f (%)	f_{cu} at 150 Times Cycle (MPa)		K_f (%)
			Sulfate Attack	Ref.		Sulfate Attack	Ref.	
S1-1	87.2	589.8	90.0	89.5	100.6	88.2	89.1	99.0
G1-1	67.3	1756.3	76.4	81.5	93.7	77.7	86.0	90.3
S1G2-1	79.0	499.9	84.9	81.5	104.2	86.7	83.7	103.6
F1S2-2	89.4	41.8	92.4	85.7	107.8	89.1	82.5	108.0
F1G2-2	72.7	1193.3	82.0	84.4	97.2	85.3	85.9	99.3
F1S2G2-2	89.5	182.4	88.5	87.1	101.6	87.3	88.4	98.8
F2S3-3	113.7	48.3	120.0	110.3	108.8	125.0	108.0	115.7
F2G3-3	77.5	708.3	87.4	89.1	98.1	89.1	91.0	98.0
F2S3G2-3	91.5	164.6	101.4	88.8	114.2	100.6	89.4	112.5
F1S2A1-2	102.8	31.3	107.7	102.0	105.6	103.5	100.6	102.9
F1G2A1-2	70.2	221.0	76.6	72.5	105.7	79.2	77.1	102.7
F1S2G2A1-2	103.9	27.4	114.1	100.0	114.1	121.0	103.2	117.2
F1S2A2-2	101.5	27.3	95.9	99.9	96.0	103.6	96.3	107.6
F1G2A2-2	85.8	184.2	85.9	81.0	106.1	89.0	86.7	102.7
F1S2G2A2-2	105.9	24.9	113.1	102.9	109.9	103.1	98.7	104.5

Meanwhile, with the increasing contents of supplementary cementitious admixtures, the decreased water to binder ratio (w/b) led to an increased strength of concrete [39,40]. As presented in Figure 2, higher compressive strength of concrete was given out by the binary use of FA and SF or the ternary use of SF, FA, and GGBS. This is contributed mainly from the highest volcano ash activity of amorphous silica of SF. Due to the lower activity of FA, the effect of FA is to reduce the strength of concrete.

**Figure 2.** Compressive strength changed with water to binder ratio.

Replacing cement with 50 kg/m^3 of AS, the compressive strength of concrete with SF and FA increased by 15.0%, and that of concrete with SF, FA, and GGBS increased by 16.1%. A slight reduction of 3.5% took place on the compressive strength of concrete with FA and GGBS. Replacing cement with 60 kg/m^3 of AS, the compressive strength of the former two concretes increased by 15.9%, while the latter one increased by 18.0%. This means that, apart from the main chemical compositions of SiO_2 and CaO , the AS with higher content of Al_2O_3 and $f\text{-CaO}$ provided good condition of secondary hydration for SF and FA, and played an expansion role in concrete due to the higher content of calcium sulfoaluminate [33,41].

3.2. Chloride Resistance

The test results of total electric flux passed through concrete samples are presented in Table 5. Overall, the total electric flux decreased with the increase of the compressive strength, as presented in Figure 3. This means that the resistance of concrete to chloride penetration was basically positive to the strength of concrete. At the same time, due to the

difference of macro- and micro- structures of concrete with pores, the resistance changed within limits, with the changes of supplementary cementitious admixtures. According to the specification of China code JGJ/T 193 for durability assessment of concrete [26], for the concretes in this experiment, the grade of resistance to chloride penetration can be divided as Q-III, Q-IV, and Q-V, respectively, corresponded to the total electric flux within 2000–1000 C, 1000–500 C, and lower than 500 C. The concretes with GGBS (specimen G1-1) or with FA and GGBS (specimen F1G2-2) belong to grade Q-III; the concretes with a little amount of SF with and without GGBS (specimens S1-1 and S1G2-1), and the concretes with FA and a larger amount of GGBS (specimen F2G3-3) belong to grade Q-IV; other concretes belong to grade Q-V.

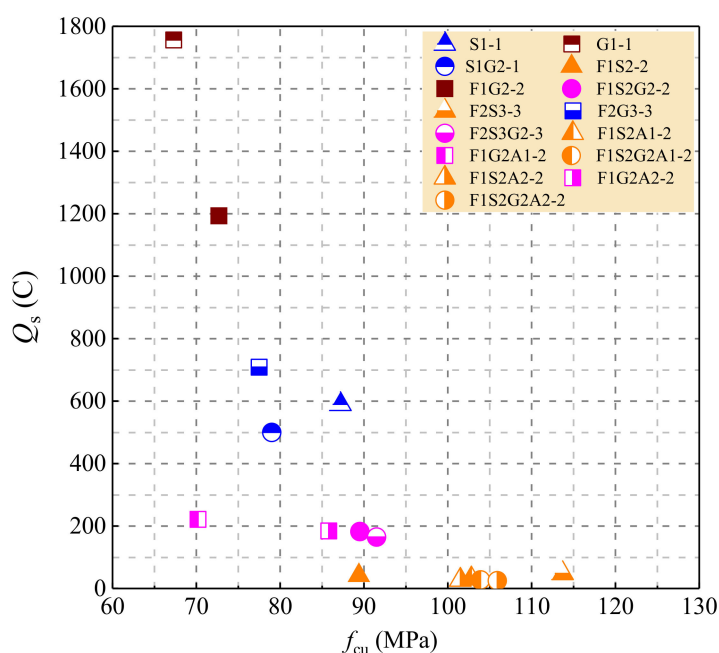


Figure 3. Total electric flux changed with compressive strength.

For the concretes at grades Q-III and Q-IV, due to the similar chemical composition of GGBS with cement, GGBS could not produce the efficiency to refine the pores pattern and distribution of concrete. Due to the filling effect and the secondary hydration of FA with the $\text{Ca}(\text{OH})_2$ produced by the hydration of cement, FA refines the pores of concrete to benefit the resistance to chloride penetration [8,13]. Although only 14 kg/m^3 of SF, about 3.2% of total weight of binders, was used, the beneficial effect of SF raised the resistance of concrete to chloride penetration from grade Q-III to Q-IV.

The concretes at grade Q-V can be further divided into two levels of Q-V-1 and Q-V-2 with the total electric flux around 200 C and below 50 C, respectively. The concretes at Q-V-1 level were all prepared with FA and GGBS and admixed with SF (specimens F1S2G2-2 and F2S3G2-3) or AS (specimens F1G2A1-2 and F1G2A2-2). The concretes at Q-V-2 level were the concretes prepared with FA and SF (specimens F1S2-2 and F1S3-3), the concretes with FA, SF, and AS, and the concretes with all kinds of admixtures used in this test. This indicates that when the GGBS was admixed, the SF or AS was needed to get a good resistance to chloride penetration; the concretes with FA and SF could reach an ideal level of resisting chloride penetration. If the GGBS was used, the AS should be admixed additionally, apart from the FA and SF. This could also improve the concrete to become the ideal level. Generally, due to the soluble C–S–H of concrete reduced by the pozzolanic effect of SF, the performance of the interfacial transition zone is improved, and the pore structure of concrete is refined. Meanwhile, the pores of concrete filled by the fine particles of SF makes concrete more compacted to eliminate continuous pores [6,8,42].

3.3. Sulfate Resistance

The test results of sulfate resistance of concrete are presented in Table 5. The sulfate corrosion resistance coefficient is basically positive to the compressive strength of concrete, as presented in Figure 4 for the concretes after 150 dry–wet cycles in a sulfate solution. The same regularity exists for the concretes after 120 dry–wet cycles in a sulfate solution. According to the specification of China codes GB 50082 and JGJ/T 193 [25,26], the grade of resistance to sulfate corrosion is determined by the maximum number of dry–wet cycles when the corrosion resistance coefficient reaches 75%. All concretes in this experiment reached the highest grade, which is larger than KS150.

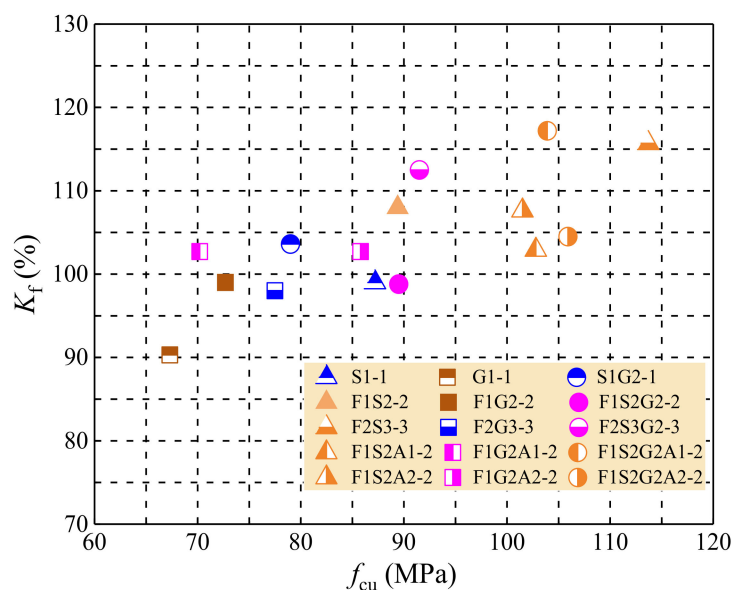


Figure 4. Sulfate corrosion resistance coefficient changed with compressive strength.

In general, the resistance of concrete to sulfate corrosion is similar to the resistance of concrete to chloride penetration, due to both of them relating to the macro- and micro structures of concrete. The grade Q-III and Q-IV concretes, including specimens G1-1, F1G2-2, S1-1, and F2G3-3, except S1G2-1, had a lower corrosion resistance coefficient than 100%. The concretes of grade Q-V had a larger corrosion resistance coefficient than 100%. This indicates that the compressive strength of concrete remained almost constant under the dry–wet recycles in a sulfate solution. In this condition, the filling effects and secondary hydration of supplementary cementitious admixtures improve the macro- and microstructures of concrete [16,18,43]; the concrete eroded layer by layer with sulfate corrosion is insignificant by the inhibited entrance of outside sulfate ions into concrete. As presented in Table 5, compared to the concrete tested at the curing age of 56 days, the compressive strength of reference concretes with GGBS and FA (specimens G1-1, F1G2-2, and F2G3-3) increased by 17.4%–27.8% at the curing age of 150 dry–wet cycles. Part of the increase of compressive strength comes directly from the strength development with the prolongation of curing age, due to the long-term increased strength of cement and the secondary hydration with pozzolanic activity of admixtures [44,45]. Others may come from the beneficial effects of filling original pores and increasing density of concrete, due the expansion of substances such as ettringite and gypsum produced by the reaction of sulfate with soluble C–S–H and layered $\text{Ca}(\text{OH})_2$ [18,46,47].

By admixing the AS, the concretes appeared to have superior ability to resist the sulfate corrosion. This meets one of the expectations of this study, to produce a high resistance of concrete to sulfate corrosion.

3.4. Frost Resistance

The frost damage of concrete is induced by the freezing and thawing cyclic action of water in pores and defects of concrete. This appears as a looseness and peeling-off of surface materials and a frost heaving damage to pores and defects of concrete. Therefore, in addition to surface freezing and thawing of concrete, the decisive effect is the infiltration of external water into the interior of the concrete [48,49]. Based on the test results of compressive strength, chloride penetration, and sulfate corrosion, five groups of concrete without SF, including G1-1, F1G2-2, F2G3-3, F1G2A1-2, and F1G2A2-2, were selected to undertake the frost test.

Figure 5 presents the test results of the relative dynamic elastic modulus and the weight loss rate of concrete. After 300 cycles of freezing and thawing, all concretes had a decrease within 5% of relative dynamic elastic modulus, and an increase within 0.4% of weight loss rate. After 300 cycles of freezing and thawing, only the concrete with GGBS (specimen G1-1) had a rapid decrease in the relative dynamic elastic modulus and a sharp increase in the weight loss rate. This agrees with the resistances of concrete to chloride penetration and sulfate corrosion. By using the FA (specimens F1G2-2 and F2G3-3), the beneficial effect of FA on the refinement of pores of concrete recovered the negative effect of GGBS. Admixing the AS accompanied with the FA and GGBS (specimens F1G2A1-2 and F1G2A2-2), no obvious effect appeared on the frost resistance of concrete.

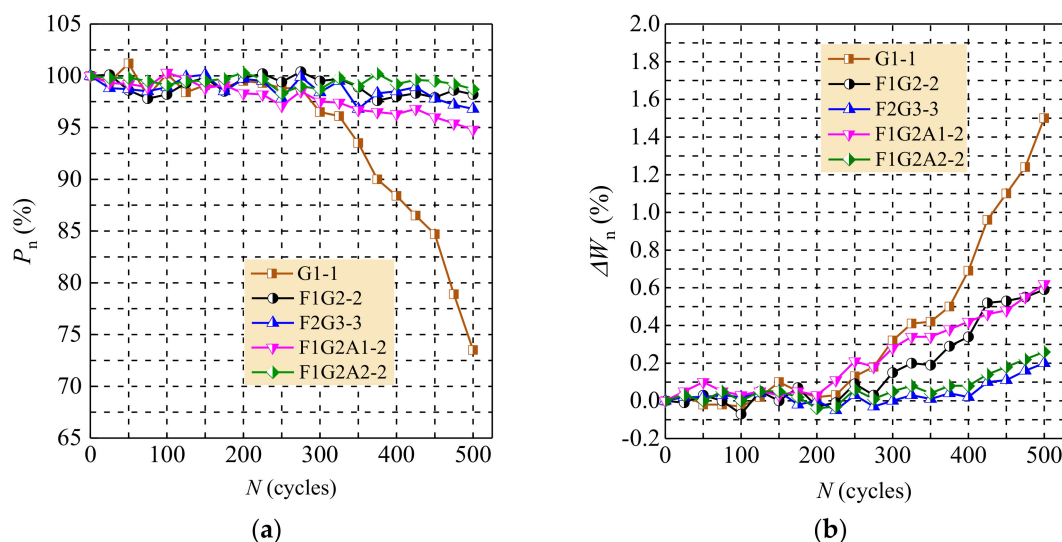


Figure 5. Changes of frost indexes of concrete: (a) relative dynamic elastic modulus; (b) weight loss.

The weight loss of specimens is mainly manifested in the damage of cementitious materials and aggregates on the surface of concrete. As per the surface morphology of specimens after 500 cycles of freezing and thawing presented in Figure 6, an obvious spalling phenomenon appeared on the surface of specimen G1-1, and some paste shedding phenomenon can be seen on surfaces of the other specimens. As seen from Figure 7, the explosion phenomena around the aggregates took place on the surface of specimen F1G2A1-2.

Figure 8 presents the changes of the relative dynamic elastic modulus and the weight loss rate with the compressive strength of concrete. High relative dynamic elastic modulus was kept with less weight loss rate for the concrete with higher compressive strength. This indicates that the high resistance of concrete to freezing and thawing was positive to the compressive strength of concrete. For concrete with at least binary cementitious admixtures including FA, SF, GGBS, and AS, the frost resistance can be comprehensively reflected by the compressive strength.

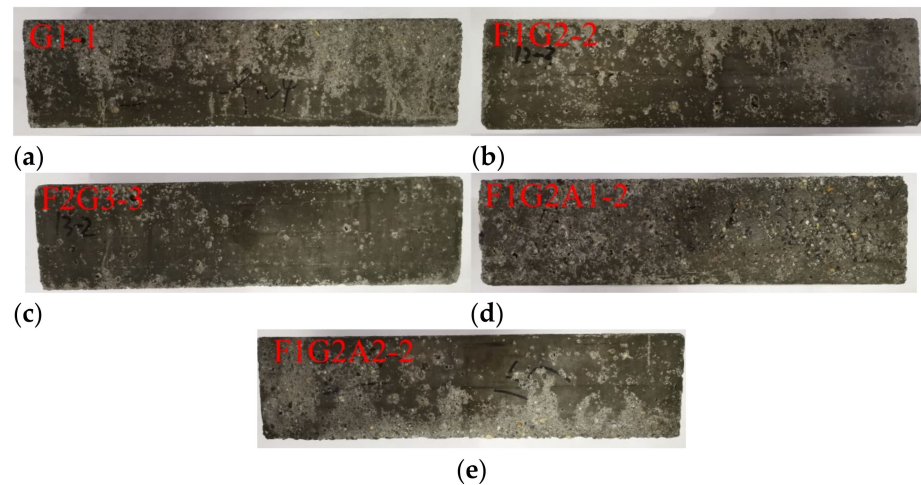


Figure 6. Appearance of specimens after 500 cycles of freezing–thawing: (a) obvious spalling on surface of G1-1; (b) paste shedding on surface of FIG2-2; (c) paste shedding on surface of F2G3-3; (d) paste shedding on surface of FIG2A1-2; (e) paste shedding on surface of FIG2A2-2.



Figure 7. Typical photo for damage of aggregate in specimen FIG2A1-2 (red circle: coarse aggregate; blue circle: fine aggregate).

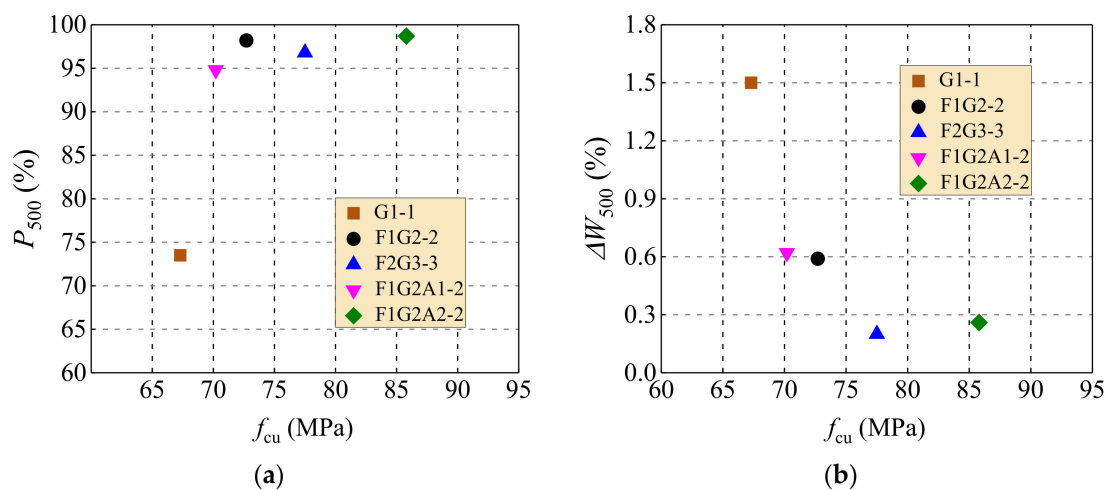


Figure 8. Frost resistance indexes of 500 cycles changed with compressive strength: (a) relative dynamic elastic modulus; (b) weight loss.

According to the specifications of China codes GB 50082 and JGJ/T 193 [25,26], the grade of the resistance of concrete to freezing and thawing is determined by the maximum number of freezing and thawing cycles, which corresponds to a relative dynamic elastic

modulus no less than 60% and a weight loss rate of no more than 5%. Therefore, all concretes in this study are at the highest grade over *F400*.

4. Conclusions

Based on the experimental study of this paper, conclusions can be made as follows:

1. Due to the difference of chemical composition, fineness, and pozzolanic activity, the supplementary cementitious admixtures present different effects on the strength and durability of concrete. In general, SF and FA benefit the compressive strength and durability of concrete, and the negative effect of GGBS can be overcome with the hybrid use of SF, FA, and AS. AS benefits the compressive strength and the resistances of concrete to chloride penetration and sulfate corrosion, while showing no obvious effect on the resistance of concrete to frost.
2. With the different combinations of the supplementary cementitious admixtures, the concrete can be produced with the compressive strength ranging from 70 MPa to 110 MPa. With the binary use of FA and SF, FA and GGBS, or the ternary use of SF, FA, and GGBS, the compressive strength of concrete increases with the reduction of water to binder ratio. With the admixing of proper content of 7% FA and 8% SF, the concrete can be prepared with compressive strength of about 100 MPa, in which the cement can be replaced by equal weight of 8% GGBS and 10~12% AS.
3. Except for the concrete only mixed with GGBS or with GGBS and FA, other concrete can be produced with ideal resistance to chloride penetration. With proper content of FA and SF, the concretes present a superior resistance to chloride penetration of the highest grade over *Q-V* with the index of total electric flux lower than 500 C specified in the China code, in which the cement can be replaced by equal weight of 8% GGBS and 10~12% AS.
4. Except for the concrete only mixed with GGBS or with GGBS and FA, other concretes reaching the highest grade over *KS150* withstood the 150 dry–wet cycles of sulfate corrosion specified in the China code. The concretes with the AS appeared to have a superior ability to resist the sulfate corrosion.
5. All concretes are at the highest grade over *F400* for the resistance to frost, with the relative dynamic elastic modulus no less than 60% and the weight loss rate no larger than 5% specified in the China code, although the concrete admixed only with GGBS appears to have a relatively low resistance.
6. The durability is positively related to the compressive strength of concrete with hybrid admixtures. With water to binder ratio of 0.29 and total binders of 500 kg/m³, the highest grades of resistances specified in the China codes to chloride penetration, sulfate corrosion, and frost can be reached for the concrete admixed with 7% FA + 8% SF + 8% GGBS or 7% FA + 8% SF + 8% GGBS + (10~12)% AS, while the compressive strength was about 100 MPa.

Author Contributions: Methodology: S.Z. and Z.R.; investigation and data curation: M.Z. (Miaomiao Zhu), X.D., and M.Z. (Mingshuang Zhao); writing: original draft preparation: M.Z. (Mingshuang Zhao), S.L., and J.D.; writing: review and funding acquisition: S.Z. and M.Z. (Miaomiao Zhu). All authors have read and agreed to the published version of the manuscript.

Funding: This research was funded by Key Scientific and Technological Research Project of University in Henan, China (19A560001, 20A560015), Postgraduate Innovation Project of NCWU (YK2019-29), State Key Research and Development Plan, China (2017YFC0703904), Innovative Sci-Tech Team of Eco-building Material, and Structural Engineering of Henan, China (YKRZ-6-066).

Institutional Review Board Statement: Not applicable.

Informed Consent Statement: Not applicable.

Data Availability Statement: The data presented in this study are contained in this article.

Conflicts of Interest: The authors declare no conflict of interest.

References

1. China Academy of Railway Sciences. *Code for Durability Design on Concrete Structure of Railway*; TB 10005-2010; China Railway Publishing House: Beijing, China, 2011.
2. Qu, F.L.; Liu, G.R.; Zhao, S.B.; Yan, L.Y. Mechanical properties of non-uniformly corroded steel bars based on length characterization. *J. Build. Mater.* **2016**, *19*, 566–570.
3. Kiese, T.S.; Bonnet, S.; Amiri, Q.; Ventura, A. Analysis of corrosion risk due to chloride diffusion for concrete structures in marine environment. *Mar. Struct.* **2020**, *73*, 102804. [[CrossRef](#)]
4. Wolfram, M.; Robin, E.; Beddoe, D.H. Sulfate attack expansion mechanisms. *Cem. Concr. Res.* **2013**, *52*, 208–215.
5. Gao, R.D.; Zhao, S.B.; Li, Q.B.; Chen, J.H. Experimental study of the deterioration mechanism of concrete under sulfate attack in wet-dry cycles. *China Civ. Eng. J.* **2010**, *43*, 48–54.
6. Wang, D.Z.; Zhou, X.M.; Meng, Y.F.; Chen, Z. Durability of concrete containing fly ash and silica fume against combined freezing-thawing and sulfate attack. *Constr. Build. Mater.* **2017**, *147*, 398–406. [[CrossRef](#)]
7. Li, Y.; Zhai, Y.; Liang, W.B.; Li, Y.B.; Dong, Q.; Meng, F.D. Dynamic mechanical properties and visco-elastic damage constitutive model of freeze-thawed concrete. *Materials* **2020**, *13*, 4056. [[CrossRef](#)] [[PubMed](#)]
8. Adorján, B. Long term durability performance and mechanical properties of highperformance concretes with combined use of supplementary cementing materials. *Constr. Build. Mater.* **2016**, *112*, 307–324.
9. Duan, P.; Shui, Z.H.; Chen, W.; Shen, C.H. Efficiency of mineral admixtures in concrete: Microstructure, compressive strength and stability of hydrate phases. *Appl. Clay Sci.* **2013**, *83–84*, 115–121. [[CrossRef](#)]
10. Nehdi, M.L.; Sumner, J. Optimization of ternary cementitious mortar blends using factorial experimental plans. *Mater. Struct.* **2002**, *35*, 495–503. [[CrossRef](#)]
11. Elahi, A.; Basheer, P.A.M.; Nanukuttan, S.V.; Khan, Q.U.Z. Mechanical and durability properties of high performance concretes containing supplementary cementitious materials. *Constr. Build. Mater.* **2010**, *24*, 292–299. [[CrossRef](#)]
12. Kojikimura, T. Enhanced hydration model of fly ash in blended cement and application of extensive modeling for continuous hydration to pozzolanic micro-pore structures. *Cem. Concr. Compos.* **2020**, *114*, 103733. [[CrossRef](#)]
13. Yan, P.Y. Mechanism of fly ash in hydration of composite cementitious materials. *J. China Ceram. Soc.* **2007**, *35(s1)*, 167–171.
14. Watcharapong, W.; Pailyn, T.; Athipong, N.; Arnon, C. Compressive strength and chloride resistance of self-compacting concrete containing high level fly ash and silica fume. *Mater. Des.* **2014**, *64*, 261–269.
15. Al-Dulaijan, S.U.; Maslehuddin, M.; Al-Zahrani, M.M.; Sharif, A.M.; Shameem, M.; Ibrahim, M. Sulfate resistance of plain and blended cements exposed to varying concentrations of sodium sulfate. *Cem. Concr. Compos.* **2003**, *25*, 429–437. [[CrossRef](#)]
16. Erhan, G.; Mehmet, G.; Erdoğan, Ö. Strength and drying shrinkage properties of self-compacting concretes incorporating multi-system blended mineral admixtures. *Constr. Build. Mater.* **2010**, *24*, 1878–1887.
17. Mohammed, S.M.; Mohamed, A.I.; El-Gamal, S.; Fitriani, H. Performances evaluation of binary concrete designed with silica fume and metakaolin. *Constr. Build. Mater.* **2018**, *166*, 400–412.
18. Liu, R.G.; Ding, S.D.; Yan, P.Y. Influence of hydration environment on the characteristics of ground granulated blast furnace slag hydration products. *B. China Ceram. Soc.* **2015**, *34*, 1594–1599.
19. Wu, M.Y.; Wang, Q.C.; Zhang, K.; Dong, Y.T.; Wang, X.L. Influence of mineral admixtures on impermeability and frost resistance of high performance concrete. *Highway* **2016**, *61*, 239–242.
20. Yan, X.L.; Gong, T.Z.; Chang, J.F.; Zheng, Y. Experimental research about sulfate resistance performance of high performance concrete. *J. Electr. Power* **2017**, *32*, 257–264.
21. Yang, B.J. Experimental Study on the Sulfate Corrosion-Resistance Admixture for Concrete. Master's Thesis, Qingdao Technological University, Qingdao, China, 2011.
22. Xu, Y.L.; Zhang, P.Y. Effect and mechanism of sulfate corrosion-resistance admixture on concrete performance. *B. China Ceram. Soc.* **2016**, *35*, 2304–2308.
23. Chang, H.L.; Mu, S.; Liu, J.Z. Influence of anticorrosion agent and curing regimes on pore structure feature and moisture loss of concrete. *J. Southeast U Nat. Sci. Ed.* **2015**, *45*, 1155–1162.
24. Liang, R. Compounding of High Durability Concrete and Application in Strong Corrosive Environment. Master's Thesis, Harbin Institute of Technology, Harbin, China, 2018.
25. Ministry of Housing and Urban-Rural Construction of the People's Republic of China. *Standard for Test Methods of Long-Term Performance and Durability of Ordinary Concrete*; GB 50082-2009; China Building Industry Press: Beijing, China, 2009.
26. Ministry of Housing and Urban-Rural Construction of the People's Republic of China. *Standard for Inspection and Assessment of Concrete Durability*; JGJ/T 193-2009; China Building Industry Press: Beijing, China, 2009.
27. Gao, R.D.; Li, Q.B.; Zhao, S.B.; Yang, X.M. Deterioration mechanisms of sulfate attack on concrete under alternate action. *J. Wuhan Univ. Technol. Sci. Ed.* **2010**, *25*, 355–359. [[CrossRef](#)]
28. Sossa, V.; Pérez-Gracia, V.; González-Drigo, R.; Rasol, M.A. Lab non-destructive test to analyze the effect of corrosion on ground penetrating radar scans. *Remote Sens.* **2019**, *11*, 2814. [[CrossRef](#)]
29. General Administration of Quality Supervision, Inspection and Quarantine of the People's Republic of China. *Common Portland Cement*; GB 175-2007; China Standard Press: Beijing, China, 2007.
30. General Administration of Quality Supervision, Inspection and Quarantine of the People's Republic of China. *Fly Ash Used for Cement and Concrete*; GB/T 1596-2017; China Standard Press: Beijing, China, 2017.

31. General Administration of Quality Supervision, Inspection and Quarantine of the People's Republic of China. *Silica Fume Cement Mortar and Concrete*; GB/T 27690-2011; China Standard Press: Beijing, China, 2011.
32. General Administration of Quality Supervision, Inspection and Quarantine of the People's Republic of China. *Ground Granulated Blast Furnace Slag Used for Cement, Mortar and Concrete*; GB/T 18046-2017; China Standard Press: Beijing, China, 2008.
33. National Development and Reform Commission of the People's Republic of China. *Sulfate Corrosion-resistance Admixtures for Concrete*; JC/T 1011-2006; China Building Materials Industry Press: Beijing, China, 2006.
34. General Administration of Quality Supervision, Inspection and Quarantine of the People's Republic of China. *Sand for Construction*; GB/T 14684-2011; China Standard Press: Beijing, China, 2011.
35. General Administration of Quality Supervision, Inspection and Quarantine of the People's Republic of China. *Pebble and Crushed Stone for Construction*; GB/T 14685-2011; China Standard Press: Beijing, China, 2011.
36. Ministry of Housing and Urban Rural Development of the People's Republic of China. *Specification for Mix Proportion Design of Ordinary Concrete*; JGJ 55-2011; China Building Industry Press: Beijing, China, 2011.
37. Ministry of Construction of the People's Republic of China. *Standard for Test Methods on Mechanical Properties of Ordinary Concrete*; GB/T 50081-2002; China Building Industry Press: Beijing, China, 2002.
38. American Society for Testing and Materials. *Standard Test Method for Electrical Indication of Concrete's Ability to Resist Chloride Ion Penetration*; ASTM C1202-19; ASTM International: West Conshohocken, PA, USA, 2019.
39. Zhao, M.L.; Ding, X.X.; Li, J.; Law, D. Numerical analysis of mix proportion of self-compacting concrete compared to ordinary concrete. *Key Eng. Mater.* **2018**, *789*, 69–75. [[CrossRef](#)]
40. Ding, X.X.; Zhao, M.L.; Zhou, S.Y.; Fu, Y.; Li, C.Y. Statistical analysis and preliminary study on the mix proportion design of self-compacting steel fiber reinforced concrete. *Materials* **2019**, *12*, 637. [[CrossRef](#)] [[PubMed](#)]
41. Li, C.Y.; Shang, P.R.; Li, F.L.; Feng, M.; Zhao, S.B. Shrinkage and mechanical properties of self-compacting SFRC with calcium sulfoaluminate expansive agent. *Materials* **2020**, *13*, 588. [[CrossRef](#)]
42. Uysal, M.; Akyuncu, V. Durability performance of concrete incorporating Class F and Class C fly ashes. *Constr. Build. Mater.* **2012**, *34*, 170–178. [[CrossRef](#)]
43. Zhao, S.B.; Li, C.Y.; Zhao, M.S.; Zhang, X.Y. Experimental study on autogenous and drying shrinkage of lightweight-aggregate concrete reinforced by steel fibers. *Adv. Mater. Sci. Eng.* **2016**, *2016*, 2589383. [[CrossRef](#)]
44. Ding, X.X.; Li, C.Y.; Xu, Y.Y.; Li, F.L.; Zhao, S.B. Experimental study on long-term compressive strength of concrete with manufactured sand. *Constr. Build. Mater.* **2016**, *108*, 67–73. [[CrossRef](#)]
45. Li, C.Y.; Wang, F.; Deng, X.S.; Li, Y.Z.; Zhao, S.B. Testing and prediction of the strength development of recycled-aggregate concrete with large particle natural aggregate. *Materials* **2019**, *12*, 1891. [[CrossRef](#)] [[PubMed](#)]
46. Gao, R.D.; Li, Q.B.; Zhao, S.B. Concrete deterioration mechanisms under combined sulfate attack and flexural loading. *J. Mater. Civ. Eng.* **2013**, *25*, 39–44. [[CrossRef](#)]
47. Gao, R.D.; Zhao, S.B.; Li, Q.B. Deterioration mechanisms of sulfate attack on concrete under the action of compound factors. *J. Build. Mater.* **2009**, *12*, 41–46.
48. Mu, R. Durability and Service Life Prediction of Concrete Subjected to the Combined Action of Freezing-Thawing, Sustained External Flexural Stress and Salt Solution. Master's Thesis, Southeast University, Nanjing, China, 2000.
49. Zhao, M.S.; Zhang, X.Y.; Song, W.H.; Li, C.Y.; Zhao, S.B. Development of steel fiber-reinforced expanded-shale lightweight concrete with high freeze-thaw resistance. *Adv. Mater. Sci. Eng.* **2018**, *2018*, 9573849. [[CrossRef](#)]